Original Article

PLCXD3-ALK, a novel *ALK* rearrangement in lung squamous cell carcinoma and its clinical responses to ALK inhibitors

Kaidi Chen[1,2#], Xiuqiong Chen[3#], Xinyue Wang[1,2#], Bing Yan[4], Aiqin Liu[4], Youhui Wang[1,2], Jing Zhou[1,2], Qianhui Wei[1,2], Yi Pan[5], Richeng Jiang[1,2,3]

[1]Tianjin Medical University Cancer Institute and Hospital, National Clinical Research Center for Cancer, Key Laboratory of Cancer Prevention on and Therapy, Tianjin's Clinical Research Center for Cancer, Tianjin, China; [2]Department of Thoracic Oncology, Tianjin Lung Cancer Center, Tianjin Cancer Institute and Hospital, Tianjin Medical University, Tianjin, China; [3]Department of Cancer Center, Daping Hospital, Army Medical University, Chongqing, China; [4]Tianjin Cancer Hospital Airport Hospital, National Clinical Research Center for Cancer, Tianjin, China; [5]Department of Pathology, Tianjin Cancer Hospital Airport Hospital, Tianjin, China

Contributions: (I) Conception and design: K Chen, X Wang; (II) Administrative support: R Jiang; (III) Provision of study materials or patients: B Yan, A Liu, Y Pan; (IV) Collection and assembly of data: J Zhou, Y Wang, Q Wei; (V) Data analysis and interpretation: X Chen; (VI) Manuscript writing: All authors; (VII) Final approval of manuscript: All authors.

[#]These authors contributed equally to this work.

Correspondence to: Richeng Jiang, MD, PhD. Tianjin Medical University Cancer Institute and Hospital, National Clinical Research Center for Cancer, Key Laboratory of Cancer Prevention on and Therapy, Tianjin's Clinical Research Center for Cancer, Huanhuxi Road, Hexi District, Tianjin 300060, China; Department of Thoracic Oncology, Tianjin Lung Cancer Center, Tianjin Cancer Institute and Hospital, Tianjin Medical University, Tianjin, China; Department of Cancer Center, Daping Hospital, Army Medical University, Chongqing, China. Email: jiangricheng@tjmuch.com; Yi Pan, MD, PhD. Department of Pathology, Tianjin Cancer Hospital Airport Hospital, Dongwu Road, Tianjin Airport Economic Area, Tianjin 300000, China. Email: tjphyLP@126.com.

Background: Lung cancer is the leading cause of cancer-related death worldwide, of which anaplastic lymphoma kinase fusion positive (*ALK*[+]) non-small cell lung cancer (NSCLC) accounts for 3-7. Here, we identified a new fusion gene *PLCXD3-ALK* (P1, A19) from a patient with advanced lung squamous cell carcinoma (LUSC) by next-generation sequencing (NGS). We aimed to evaluate its oncogenic potential by performing functional studies *in vitro* and tumorigenicity *in vivo* of this fusion protein.

Methods: We performed functional experiments in NIH-3T3 cells with stable expression of *PLCXD3-ALK* including soft agar colony formation assay, cell proliferation and viability assays, and transwell assay. The activation of downstream pathways and the response to ALK inhibitors crizotinib and alectinib were demonstrated by western blotting (WB). In addition, we further evaluated the tumorigenicity of the *PLCXD3-ALK* mutants in nude mice.

Results: Similar to *EML4-ALK*, the *PLCXD3-ALK* fusion promoted proliferation and the capacity for non-anchorage-dependent growth of NIH-3T3 cells. We demonstrated that *PLCXD3-ALK* can activate ALK self-phosphorylation and downstream pathways, which could be inhibited by the addition of ALK inhibitors. Moreover, we observed that this gene could provoke oncogenic transformation in nude mice. Meanwhile, the patient was monitored for disease progression with computed tomography (CT) scanning during treatment with alectinib, and a benefit was observed.

Conclusions: We identified and functionally validated *PLCXD3-ALK* as a novel rare fusion in NSCLC that has not been previously reported. It can serve as a meaningful therapeutic target for ALK inhibitors of *ALK*[+] NSCLC.

Keywords: Non-small cell lung cancer (NSCLC); *PLCXD3-ALK* fusion; anaplastic lymphoma kinase inhibitors (ALK inhibitors); targeted therapy

Submitted Aug 30, 2024. Accepted for publication Dec 06, 2024. Published online Jan 21, 2025.
doi: 10.21037/jtd-24-1428
View this article at: https://dx.doi.org/10.21037/jtd-24-1428

Introduction

Lung cancer has been widely concerned due to its high morbidity and mortality, of which non-small cell lung cancer (NSCLC) accounts for 85% (1). Rearrangements of the anaplastic lymphoma kinase (*ALK*) gene account for approximately 3–7% of NSCLC, with the most common fusion partner being *EML4* (2). The 5' partner might influence the intrinsic properties of the fusion protein through changing the kinase activity, protein stability, transformative potential, and drug sensitivity *in vitro* (3). Different *ALK* fusion proteins can mediate different signaling pathways, resulting in different sensitivity and resistance to ALK tyrosine kinase inhibitors (TKIs) (4). Small molecule TKIs blocking the aberrant ALK signaling pathway and binding to tyrosine kinase receptors have been shown to be an effective way to inhibit the growth of *ALK*$^+$ cancer cells (5). ALK TKIs have emerged as the standard treatment for patients harboring *ALK* gene rearrangements in advanced NSCLC. With the advancement of ALK TKIs, there are now three generations of these targeted therapies (6). The first-generation drug, crizotinib, revolutionized the treatment landscape (7). Subsequently, second-generation TKIs such as brigatinib, alectinib, ceritinib, and ensartinib were developed to overcome resistance issues, showing improved patient outcomes in clinical trials. The third-generation TKI, lorlatinib, which has also demonstrated remarkable efficacy and safety profiles in clinical studies (8,9). These agents have been approved for the first-line treatment of *ALK*$^+$ advanced NSCLC, offering patients a spectrum of treatment options tailored to their specific needs and therapeutic responses (10). In a recent study, the fourth-generation ALK inhibitor NVL-655 demonstrated potent inhibitory effects against a range of ALK resistance mutations, including the G1202R mutation. NVL-655 shows high brain penetration, making it effective for patients with brain metastases. Additionally, it exhibits minimal inhibition of the f tropomyosin receptor kinase (TRK) family, potentially reducing TRK-related central nervous system side effects (11). Previously, a total of 92 *ALK* fusion partners identified until 2020 were summarized by Ou *et al.* (12). We further summarized the *ALK* fusion partners newly discovered in lung cancer patients including 44 *ALK* fusion partners and 13 intergenic rearrangements to *ALK* (*Table 1*). Overall, about 136 distinct *ALK* fusion partners have been identified in literatures (by the end of March 2024). Most of these novel *ALK* fusion variants were shown to be *ALK*$^+$ by immunohistochemistry (IHC) and the patients who harbored these *ALK* arrangements had been reported to be obviously sensitive to ALK TKIs (*Table 1*). *ALK* fusions result in ligand-independent dimerization and hyperactivation of pro-mitogenic and anti-apoptotic signaling including JAK-STAT, PI3K-AKT, and RAS-MAPK pathways. Each of these pathways plays a crucial role in regulation of various cellular processes, including proliferation, survival, differentiation, and migration (13-15). In our clinical setting, we identified a novel *ALK* fusion partner, *PLCXD3*, in a NSCLC patient by next-generation sequencing (NGS). Subsequently, we demonstrated that the *PLCXD3-ALK* fusion gene had similar kinase activity to *EML4-ALK* through *in vitro* functional experiments and *in vivo* tumor-forming experiments. The patient with *PLCXD3-ALK* fusion was dramatically sensitive to ALK inhibitors, which further manifested that *PLCXD3-ALK* is an available therapeutic target for ALK inhibitors. We present this article in accordance with the ARRIVE reporting checklist (available at https://jtd.amegroups.com/

Highlight box

Key findings

- A new rare anaplastic lymphoma kinase (*ALK*) fusion, *PLCXD3-ALK*, was identified in a lung squamous cell carcinoma patient. *PLCXD3-ALK* is a potential therapeutic target for ALK inhibitors, as demonstrated *in vitro* and *in vivo*.

What is known and what is new?

- *ALK* gene rearrangements account for 3–7 of non-small cell lung cancer, with an increasing number of rare *ALK* fusions detected. These fusions can activate different signaling pathways, affecting sensitivity and resistance to ALK inhibitors.
- Our study showed that *PLCXD3-ALK* exhibits similar functional characteristics to *EML4-ALK* through *in vitro* and *in vivo* experiments.

What is the implication, and what should change now?

- *PLCXD3-ALK* is a viable therapeutic target for ALK inhibitors, and its inclusion in clinical diagnosis and targeted therapy protocols is recommended.

Table 1 The ALK fusion partners were newly found in lung cancer from March 2020 to March 2024

No.	Fusion partner	Chromosomal location	Fusion breakpoint	Response to ALK TKIs	Method of detection	Variant frequency (%)	FISH/IHC	Pathological type	Author [year]
1	*LTBP1*	2p22.3	NR	PR to crizotinib	NGS	NR	ND/+	NSCLC-LUAD	Qian [2020]
		2p22.3	(L3, A19)	PR to crizotinib	NGS	10.28	NR/NR	NSCLC-LUAD	Ning [2021]
2	*NLRC4*	2p22.3	(N6, A20)	PR to crizotinib	NGS	24.44	ND/ND	NSCLC-LUAD	Wu [2020]
3	*HPCAL1*	2p25.1	(H1, A20)	PR to crizotinib	NGS	1.87	+/+	NSCLC-LUAD	Wang [2020]
4	*CCNY*	10p11.21	(C1:A20)	PR to crizotinib	NGS	16.64	+/+	NSCLC	Wu [2020]
5	*ATIC*	2q35	(A7:A20)	PR to crizotinib	NGS	16.33	+/+	NSCLC	Wu [2020]
6	*PNPT1*	2p16.1	(P19, A19)	PR to crizotinib	NGS	NR	ND/+	NSCLC-LUAD	Jin [2020]
7	*TMED2*	12q24.31	(T4, A20)	NR	NGS	NR	+/+	NSCLC-LUAD	Mao [2020]
8	*COX7A2L*	2p21	(C2, A20)	PR to ceritinib	NGS	11.61	ND/+	NSCLC-LUAD	Jiao [2021]
9	*RMDN2*	2p22.2	(R2, A15)	NR	NGS	NR	+/NR	NSCLC-LUAD	Jiang [2021]
10	*NBEA*	13q13.3	(N5, A20)	PR to alectinib	NGS	19.65	+/+	NSCLC-LUAD	Liang [2021]
11	*SLC8A1*	2p22.1	(S2, A19)	PR to crizotinib	NGS	5.98	+/ND	NSCLC-LUAD	Zhu [2021]
		2p22.1	(S2, A20)	PR to alectinib	NGS	10.39	ND/+	NSCLC-LUAD	Deng [2022]
12	*LRRC4C*	11p12	(L1, A19)	PR to crizotinib	NGS	NR	ND/+	NSCLC-LUAD	Wang [2021]
13	*GHR*	5p13.1-p12	(G1, A20)	PR to crizotinib	NGS	NR	ND/+	NSCLC-LUAD	Pan [2021]
14	*PDK1*	2q31.1	(P7, A20)	PR to alectinib	NGS	12.85	ND/+	NSCLC-LUAD	Zeng [2021]
15	*LOC285000*	2q12.2	NR	PR to crizotinib; SD to alectinib	NGS	1.00	ND/ND	NSCLC-LUAD	Zhang [2021]
16	*THUMPD2*	2p22.1; 2p22-p21	(T6, A20)	PR to crizotinib	NGS	6.20	ND/+	NSCLC-LUAD	Wang [2021]
17	*STK3*	8q22.2	(S6, A20)	PR to crizotinib, SD to alectinib	NGS	3.10	ND/+	NSCLC-LUAD	Feng [2021]
18	*GPC1*	2q37.3	(G1, A20)	NR	RNA sequencing	NR	+/ND	PSC	Xiong [2021]
19	*PLB1*	chromosome: XIII	(P56, A20)	SD to ceritinib	NGS	28.33	+/+	LCNEC	Wang [2021]
20	*SMPD3*	16q22.1	(S1, A20)	NR	NGS	NR	+/+	NSCLC-LUAD	Liang [2021]
21	*PARD3*	10p11.22-p11.21	(P22, A20)	NR	NGS	7.18	ND/+	NSCLC-LUAD	Yang [2021]
22	*GPR75-ASB3*	2p16.2	(G1, A20)	NR	NGS	NR	ND/+	NSCLC-LUAD	He [2021]
23	*SETD3*	14q32.2	(S6, A20)	PR to crizotinib	NGS	36.03	ND/+	NSCLC-LUAD	Dai [2022]

Table 1 (*continued*)

Table 1 (*continued*)

No.	Fusion partner	Chromosomal location	Fusion breakpoint	Response to ALK TKIs	Method of detection	Variant frequency (%)	FISH/IHC	Pathological type	Author [year]
24	*CCDC85A*	2p16.1	(C2, A20)	PR to alectinib	NGS	NR	ND/+	NSCLC-LUAD	Lin [2022]
25	*SDK1*	7p22.2	(S36, A20)	PR to SAF-189s	NGS	9.20	ND/+	NSCLC-LUAD	Ma [2022]
26	*LMO7*	13q22.2	(L15, A20)	PR to crizotinib	NGS	NR	ND/ND	NSCLC-LUAD	Yang [2022]
27	*HLA-DRB1*	6p21.32	(H8, A20)	PR to crizotinib, ceritinib	NGS	NR	ND/ND	NSCLC-LUAD	Peng [2022]
28	*CTNND1*	11q12.1	(C14, A20)	PR to alectinib	NGS	NR	ND/+	NSCLC-LUAD	Tian [2022]
29	*SSFA2*	chromosome: 7	(S8, A20)	CR to alectinib	NGS	NR	+/+	NSCLC-LUAD	Lin [2022]
30	*CPE*	4q32.3	(C6, A20)	PR to alectinib	NGS	NR	ND/+	NSCLC-LUAD	Qin [2022]
31	*DHX8*	17q21.31	NR	NR	NGS	NR	ND/ND	NSCLC-LUAD	Wang [2022]
32	*RNF144A*	2p25.1	(A19, R9)	PR to alectinib; no response to TGRX-326	NGS	36.98	ND/+	NSCLC-LUAD	Li [2023]
33	*KIF13A*	6p22.3	(K18, A20)	PR to alectinib	NGS	11.40	+/+	NSCLC-LUAD	Mo [2023]
34	*LIMS1*	2q12.3	(L1, A20)	no response to crizotinib	NGS	NR	ND/+	NSCLC-LUAD	Shi [2023]
35	*RSRC1*	3q25.32	(R6: A20)	NR	NGS	NR	ND/ND	NSCLC	Xia [2023]
36	*PPFIA1*	11q13.3	(P2, A20)	SD to alectinib	NGS	10.00	ND/+	NSCLC-LUAD	Yan [2023]
37	*INTS10*	8p21.3	(I18, A20)	PR to crizotinib	NGS	25.85	+/ND	NSCLC-LUAD	Zhai [2023]
38	*KIDINS220*	2p25.1	NR	PR to alectinib	NGS	NR	ND/+	NSCLC-LUAD	Lei [2023]
39	*SLC34A2*	4p15.2	(S1, A15)	PR to alectinib	NGS	NR	ND/+	NSCLC-LUAD	Zhou [2023]
40	*CACNA1D*	3p21.1	(C3, A19)	PR to alectinib	NGS	16.9	ND/+	NSCLC-LUAD	Xie [2024]
41	*LOC399815*	10q26.13	(L5, A20)	PR to alectinib	NGS	8.16	ND/+	NSCLC-LUAD	Li [2024]
42	*INPP5D*	2q37.1	(I2, A19)	PR to alectinib	NGS	13.92	ND/ND	NSCLC-LUAD	Li [2024]
43	*KANK1*	9p24.3	(K3, A20)	PR to alectinib	NGS	12.58	ND/ND	NSCLC-LUAD	Tang [2024]
44	*UGP2*	2p15	NR	PR to alectinib	NGS	NR	ND/+	NSCLC-LUAD	Chen [2024]
Intergenic region fusion									
1	*LINC00478*	Chr 21:18,166,634	(L: between LINC00478 and LINC01549, A20)	PR to alectinib	NGS	NR	ND/ND	NSCLC-LUAD	Peng [2020]
2	*MRPS9*	2q12.1	(M: upstream MRPS9, A19)	PR to crizotinib, alectinib	NGS	NR	ND/ND	NSCLC-LUAD	Zhou [2021]
3	*CDCA7*	2q31.1	(C: intergenic, A20)	PR to crizotinib	NGS	22.68	ND/+	NSCLC-LUAD	Zhao [2021]
4	*FSIP2*	2q32.1	(C: intergenic, A19)	PR to crizotinib	NGS	24.06	ND/+	NSCLC-LUAD	Zhao [2021]

Table 1 (*continued*)

Table 1 (*continued*)

No.	Fusion partner	Chromosomal location	Fusion breakpoint	Response to ALK TKIs	Method of detection	Variant frequency (%)	FISH/IHC	Pathological type	Author [year]
5	*LRRC1*	6p12.1	(L: between KLHL31 and LRRC1, A20)	PR to ensartinib	NGS	NR	ND/+	NSCLC-LUAD	Qiu [2021]
6	*F3*	1p21.3	(F: between F3 and SLC44A3, A20)	NR	NGS	3.86	ND/+	NSCLC-LUAD	Chen [2021]
7	*HIVEP1*	6p24.1	(H: upstream HIVEP1, A20)	PR to alectinib	NGS	7.60	+/+	NSCLC-LUAD	Gu [2022]
8	*GCKR*	2p23.3	(G: upstream C2 or F16, A20)	SD to dabrafenib plus trametinib combined with alectinib	NGS	9.70	ND/+	NSCLC-LUAD	Liao [2022]
9	*LINC02010*	3q24	(L: downstream ZIC4, A20)	no response to alectinib	NGS	22.60	ND/+	NSCLC-LUAD	Liao [2022]
10	*RMST*	12q23.1; 12q21	(R: 5'-UTR, A20)	PR to ceritinib	NGS	NR	ND/+	NSCLC-LUAD	Li [2022]
11	*ARHGAP5*	14q12	(A: downstream of ARHGAP5, A20)	PR to alectinib	NGS	NR	ND/ND	NSCLC-LUAD	Cheng [2022]
12	*LOC101927967*	2p12	(L: downstream intergenic, A20)	NR	NGS	13.35	+/+	NSCLC-LUAD	Jia [2022]
13	*LINC01923*	2q33.1	(L: intergenic, A20)	PR to ensartinib	NGS	27.94	+/+	NSCLC-LUAD	Wang [2023]

ALK, anaplastic lymphoma kinase; TKIs, tyrosine kinase inhibitors; FISH, fluorescence in situ hybridization; IHC, immunohistochemistry; NR, not reported; PR, partial response; NGS, next-generation sequencing; ND, not done; NSCLC, non-small cell lung cancer; LUAD, lung adenocarcinoma; SD, stable disease; PSC, pulmonary sarcomatoid carcinoma; LCNEC, lung large-cell neuroendocrine carcinoma; CR, complete response; UTR, untranslated region.

article/view/10.21037/jtd-24-1428/rc) (16).

Methods

Clinical sample

The patient had signed an informed consent form to agree to the collection of specimens and genetic testing. The study was conducted in accordance with the Declaration of Helsinki (as revised in 2013). The study was approved by the Ethics Committee of Tianjin Medical University Cancer Institute and Hospital (No. bc20240063) and informed consent was taken from the patient. NGS testing was conducted by the Center for Precision Cancer Medicine & Translational Research of Tianjin Medical University Cancer Institute and Hospital. During the therapy, tumor size, and peripheral obstructive inflammation were monitored dynamically using computed tomography (CT) scans every 2–3 months.

Cell culture

The cell line NIH-3T3 was purchased from Wuhan Pricella Biotechnology Co., Ltd. (Wuhan, China). The 293T was obtained from the American Type Culture Collection (ATCC). Both NIH-3T3 and 293T were cultured in Dulbecco's modified Eagle's medium (DMEM) supplemented with 10% fetal bovine serum (FBS; EXCELL, Suzhou, China) and 1% penicillin and streptomycin (Solarbio, Beijing, China). Cells underwent <10 passages post-revival, were mycoplasma-free following monthly testing and were incubated under 37 ℃, 5% CO_2. Prior to performing experiments such as western blotting (WB), cell proliferation, and viability assays, cells were serum-starved for 24 hours.

Construction of stable cell lines

The pLVX-IRES-Puro-PLCXD3-ALK, pLVX-IRES-Puro-EML4-ALK, and corresponding pLVX vector constructs were engineered by GENEWIZ (a division of Azenta Life Sciences, Suzhou, China). To generate lentivirus, 293T cells were co-transfected with pLVX-puro EML4-ALK or PLCXD3-ALK plasmids and packaging plasmids using Lipo2000 Transfection Reagent (Thermo Fisher Scientific, Waltham, MA, USA). Forty-eight hours post-transfection, the virus-containing supernatant was harvested. These lentiviruses were then administered to the NIH-3T3 cells for transfection for 48 hours, followed by selection with puromycin (2 μg/mL). Thereafter, transduced cells were used for further analysis.

IHC of the stable cell lines

Cell culture slides were prepared in advance. After blocking endogenous peroxidase activity, the primary antibody was applied overnight at 4 ℃. The sections were incubated with anti-ALK rabbit polyclonal antibody (Proteintech #24184-1-AP; Proteintech, Wuhan, China) at 4 ℃ overnight. They were then incubated with secondary antibody for 30 min at room temperature. The sections were counterstained with diaminobenzidine (DAB) for 3 min followed by the appearance of brown staining. Hematoxylin was applied to stain the nucleus for 10 min. Cytoplasmic staining was considered positive for ALK.

WB analysis

Cells were lysed in radioimmune precipitation assay (RIPA) buffer containing proteinase inhibitor cocktail (Roche, Basel, Switzerland) and one phosphatase inhibitors (Thermo Fisher Scientific). Quantify the lysate using the Pierce BCA Protein Assay Kit (Thermo Fisher Scientific). Total proteins were separated with sodium dodecyl sulfate-polyacrylamide gel electrophoresis (SDS-PAGE) gels, and transferred onto a polyvinylidene fluoride (PVDF) membrane. The membrane were incubated with primary antibodies overnight at 4 ℃. The antibodies used were purchased from Cell Signaling Technology (Beverly, MA, USA) [human phosphorylated ALK (pY1604) (#3341s), ALK (#3633s), phosphorylated ERK (#4370s), ERK (#4695s), phosphorylated STAT3 (#9145s), STAT3 (#9139s), phosphorylated AKT (#4060s), and AKT (#9272s)]. The glyceraldehyde 3-phosphate dehydrogenase (GADPH) antibody was from Abclonal (Wuhan, China) (#AC033). Then, the secondary antibody was used to incubate for 60 min at room temperature. Finally, specific proteins were detected using Western Lightning Plus-ECL (Millipore Corporation, Billerica, MA, USA).

Soft agar colony formation assay

One low melting point agarose (containing 20% FBS in DMEM) was placed on the bottom of the culture plate and solidified at room temperature for 30 min. Next, 0.7% low melting point agarose (containing 20% FBS in DMEM)

was applied to suspended cells and then gently added the suspension to the bottom. The plates were cultured under 37 ℃, 5% CO_2 for 3 weeks. Colonies larger than 50 μm were counted and analyzed. The experiment was repeated three times.

Cell proliferation and cell viability assays

Culture cells under starvation conditions for 24 hours. 1×10^3 cells/well in 96-well plates were cultured for 24 hours before exposure to various concentrations of drugs for 72 hours. Cell counting kit-8 (APExBIO #K1018; APExBIO, Houston, TX, USA) reagent was added to each well according to the manufacturer's instructions. Each assay was repeated three times.

Transwell assay

Transwell chambers with or without Matrigel were used to perform cell invasion or migration assays. 3×10^4 cells suspended in serum-free DMEM medium were added to the upper chamber of each 24-well culture inserts and DMEM with 20% FBS was placed to the lower chamber. The cells were incubated at 37 ℃ for 24 hours, then we removed the cells retained on the upper side of the chamber, and the cells pass through the membrane were fixed in four paraformaldehyde and stained with crystal violet, the migrated or invaded cells were counted and analyzed.

In vivo experiments

Six-week-old nude mice (Gempharmatech Co., Ltd., Nanjing, China) were maintained in a specific pathogen-free animal facility. The mice were randomly divided into seven groups and subcutaneously implanted into the back region with 1×10^7 cells. The mice were orally administered vehicle, crizotinib (50 mg/kg/2 days, Selleck, Houston, TX, USA), or alectinib (10 mg/kg/2 days, Selleck) after tumor formation. Tumor volume were measured every 3 days and calculated as follows: tumor volume = $\pi \times (\text{width})^2 \times \text{length}/6$. The mice were euthanized at the end of the experiment or when the humane endpoints of animal ethics were reached. Experiments were performed under a project license (No. 2024006) granted by the Animal Care and Use Committee of Tianjin Medical University Cancer Institute and Hospital, in compliance with institutional guidelines for the care and use of animals.

Statistical analysis

Two-tailed Student's unpaired *t*-test and analysis of variance (ANOVA) were used to compare the differences of average values *in vitro* experiments and the size of xenografted tumors *in vivo*. Data were expressed as the mean ± standard deviation (SD). A two-sided P value <0.05 was considered to indicate statistical significance.

Results

Detection of a rare ALK fusion

A 45-year-old non-smoking female patient was diagnosed with stage IV lung squamous cell carcinoma (LUSC). IHC: P40 (+), P63 (+), CK5/6 (+), CK7 (–), TTF1 (–), NapsinA (–) (*Figure 1A*). Then, the NGS testing of the tumor was performed, and the mutation profile revealed the presence of a novel rearrangement between chromosomes 2 and 5, with a mutation allele frequency of 45.99 (*Figure 1B*). Additionally, high ALK expression was detected by Ventana IHC-ALK (D5F3) assay and fluorescence in situ hybridization (FISH) of ALK further confirmed ALK rearrangement (*Figure 1C*,*1D*). This fusion gene was composed of exon 1 of *PLCXD3* and exons 19–29 of *ALK*, which retained the kinase domain of ALK, and was presumed to lead to oncogenic activation of ALK (*Figure 1E*). To identify that *PLCXD3-ALK* was the driving force in tumor progression, we further performed functional studies of this fusion protein.

PLCXD3-ALK activates downstream signaling pathways

To investigate the oncogenic function of *PLCXD3-ALK*, we constructed expression plasmids for *PLCXD3-ALK* and *EML4-ALK*. Next, we established NIH-3T3 cells that stably expressed *PLCXD3-ALK* (PLCXD3-ALK/3T3), *EML4-ALK* variant 1 (positive control, EML4-ALK/3T3), *ALK* WT(negative control, ALK WT/3T3) and the pLVX-IRES-Puro vector only (mock) transfected cells (pLVX/3T3). By comparing *PLCXD3-ALK*'s function with that of the *EML4-ALK* fusion, we aimed to assess the importance of PLCXD3 as a novel fusion protein. To demonstrate that *ALK* expression occurred in *ALK*-rearranged cells, we observed that the ALK WT/3T3, PLCXD3-ALK/3T3 and EML4-ALK/3T3 cells were positive for ALK by IHC, whereas the mock cells were negative (*Figure 2A*). We observed the phosphorylation of the ALK kinase domain Tyr1604 site

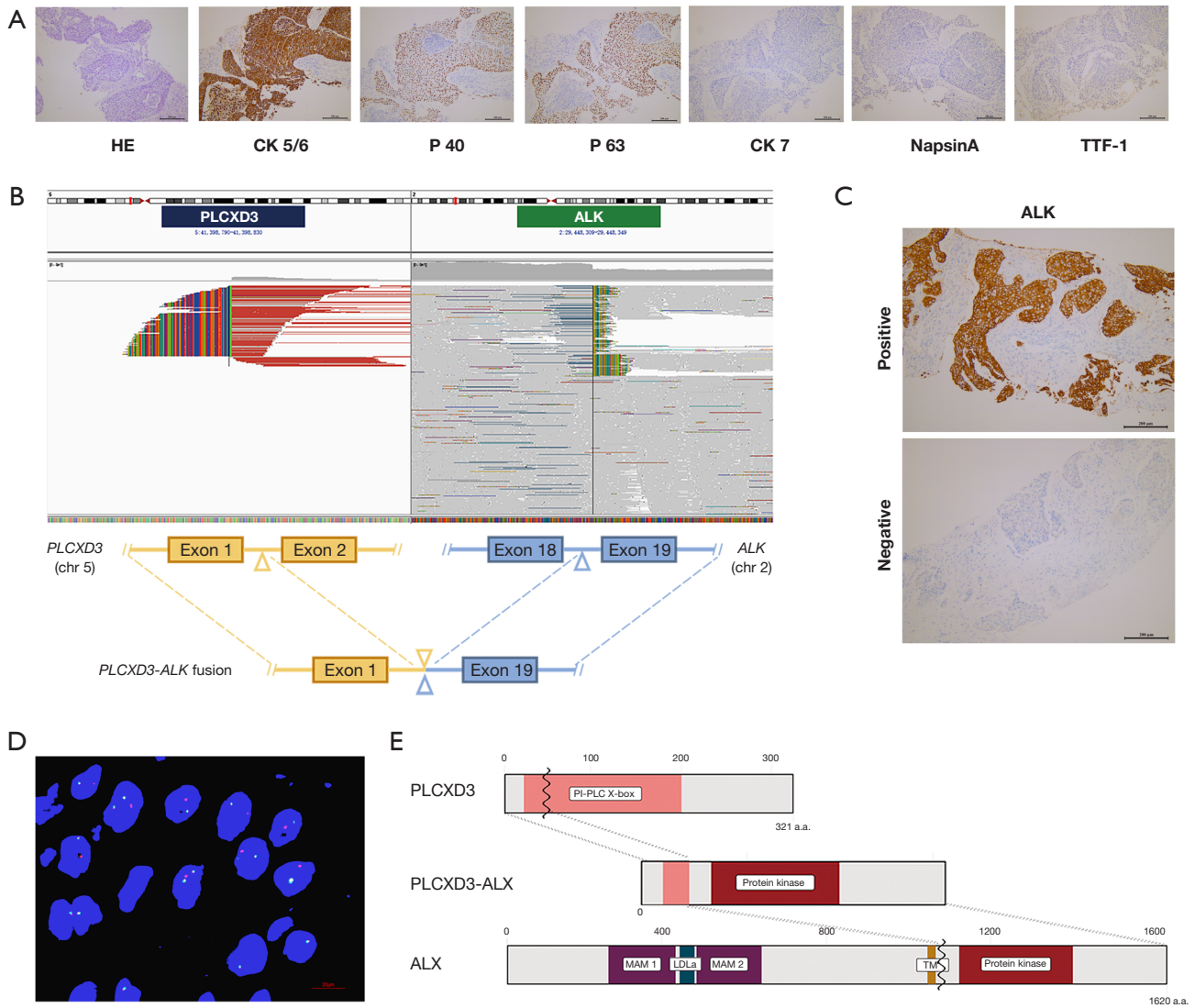

Figure 1 Histological findings from biopsy specimen and identification of the PLCXD3-ALK fusion in a lung cancer patient. (A) Pathological examination of the patient. HE staining was performed to evaluate the histopathological features of tumor tissues. IHC staining of tumor tissue showed positive for CK5/6, P40, P63 and negative for CK7, Napsin A, TTF-1 (×10), which showed squamous cell lung cancer. (B) *PLCXD3-ALK* fusion in the present case visualized using the IGV. (C) Ventana IHC-ALK (D5F3) detection of *ALK* expression (×10). (D) FISH analysis utilizing the ALK split apart probe, demonstrating distinct split signals suggestive of a rearrangement of the *ALK* gene. Images were captured using a Leica DM5500B fluorescence microscope and analyzed with CytoVision software. The green signals, orange signals and yellow signals represent the 5'-*ALK* gene, 3'-*ALK*, and intact *ALK* gene respectively. (E) Hypothesized structure of the dimerized PLCXD3-ALK fusion protein. PLCXD3 contains a PI-PLC X-box domain [22–197] (upper panel). Residues corresponding to *PLCXD3* and *ALK* were shown. Protein domain diagrams illustrating the preservation of the C-terminal tyrosine kinase domain of ALK in the PLCXD3-ALK fusion protein (middle panel). The structure of the native human ALK receptor protein-tyrosine kinase (lower panel). The extracellular segment (residues 19–1,038) of *ALK* contains two MAM components (264–427 and 480–626), and an LDLa domain [453–471]. A transmembrane segment (residues 1,039–1,059) connects the extracellular domain with the intracellular domain [1,060–1,620], which contains the PK domain [1,116–1,392]. HE, hematoxylin and eosin; ALK, anaplastic lymphoma kinase; IHC, immunohistochemistry; IGV, Integrative Genomics Viewer; FISH, fluorescence in situ hybridization; MAM, mitochondria-associated membrane; PK, protein kinase.

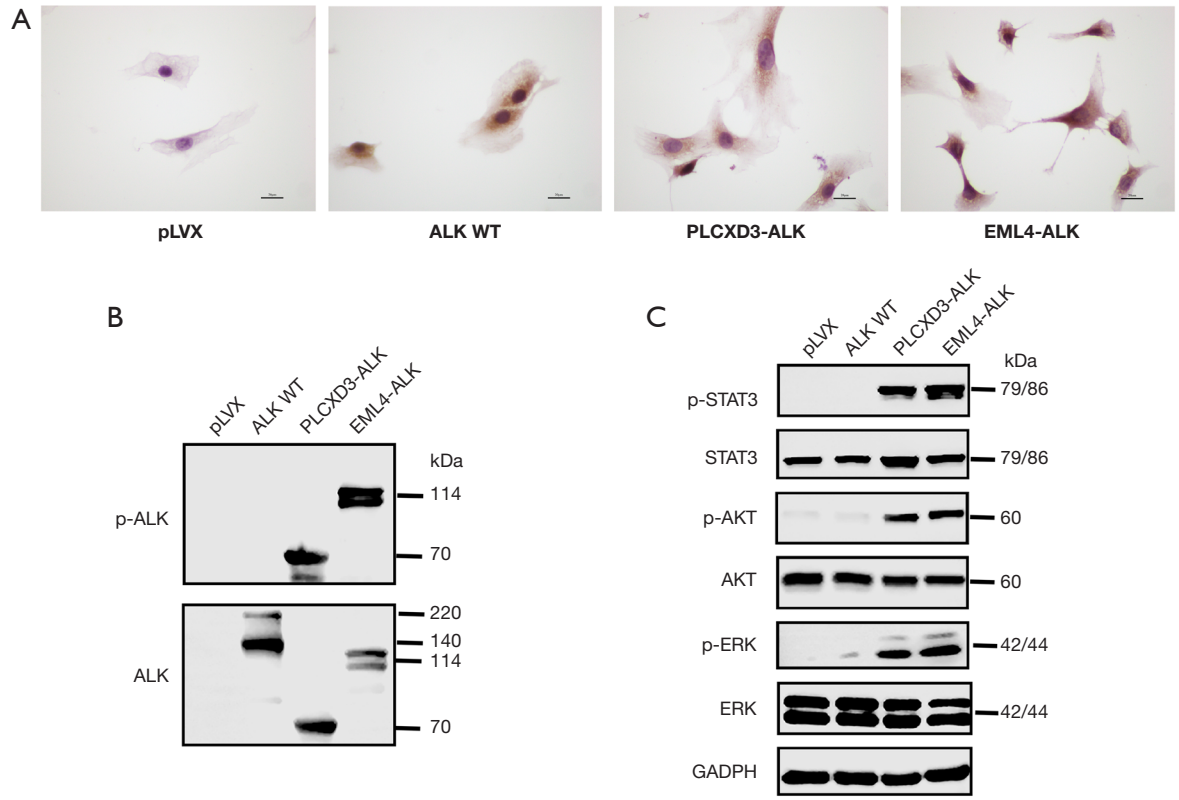

Figure 2 *PLCXD3-ALK* activated downstream signaling pathways. (A) ALK IHC images of transfected cells using the ALK antibody. Images were captured using an Olympus microscope. (B) Self-phosphorylation and (C) activation of downstream signaling pathways by the *PLCXD3-ALK* fusion. Cell lysates were subjected to SDS-PAGE and immunoblotting analysis with specific antibodies. Experiments were repeated three times. Once representative experiment is shown here. ALK, anaplastic lymphoma kinase; WT, wild type; p-, phosphorylated-; GADPH, glyceraldehyde 3-phosphate dehydrogenase; IHC, immunohistochemistry; SDS-PAGE, sodium dodecyl sulfate-polyacrylamide gel electrophoresis.

in both PLCXD3-ALK/3T3 and EML4-ALK/3T3 cells, indicating that both ALK fusion proteins were constitutively activated (*Figure 2B*). Next, we analyzed the downstream signaling pathways that might be affected by the *PLCXD3-ALK* fusion. The results indicated that in NIH-3T3 cells transfected with *PLCXD3-ALK* and *EML4-ALK*, there was a significant increase in the phosphorylation of STAT3, AKT, and ERK compared to cells transfected with the empty vector (*Figure 2C*).

Oncogenic properties of PLCXD3-ALK

Next, we used a soft agar colony formation assay to determine whether the 5' partner, *PLCXD3*, affects transformation and proliferation. As expected, the NIH-3T3 cells transfected with *PLCXD3-ALK* formed a considerable number of colonies in soft agar. Although the number of colonies was less than that of the NIH-3T3 cells transfected with *EML4-ALK*, it was still sufficient to show their capacity for non-anchorage-dependent growth. In contrast, the cells expressing the empty vector did not generate a comparable number of colonies (*Figure 3A*). Similarly, in the cell proliferation assay, we also observed similar results, with the transfection of *PLCXD3-ALK* significantly enhancing the proliferation capacity of NIH-3T3 cells (*Figure 3B*). Moreover, this proliferative capacity can be significantly inhibited by ALK TKIs (*Figure 3C*). We assessed cell viability following treatment with varying concentrations of ALK TKIs. The results demonstrated that PLCXD3-ALK and EML4-ALK exhibit comparable sensitivity to alectinib and crizotinib (*Figure 3D*). Furthermore, our findings from the transwell assay demonstrated a significant enhancement in the *in vitro* migration and invasive capacity of cells expressing *PLCXD3-ALK* than that of the negative control

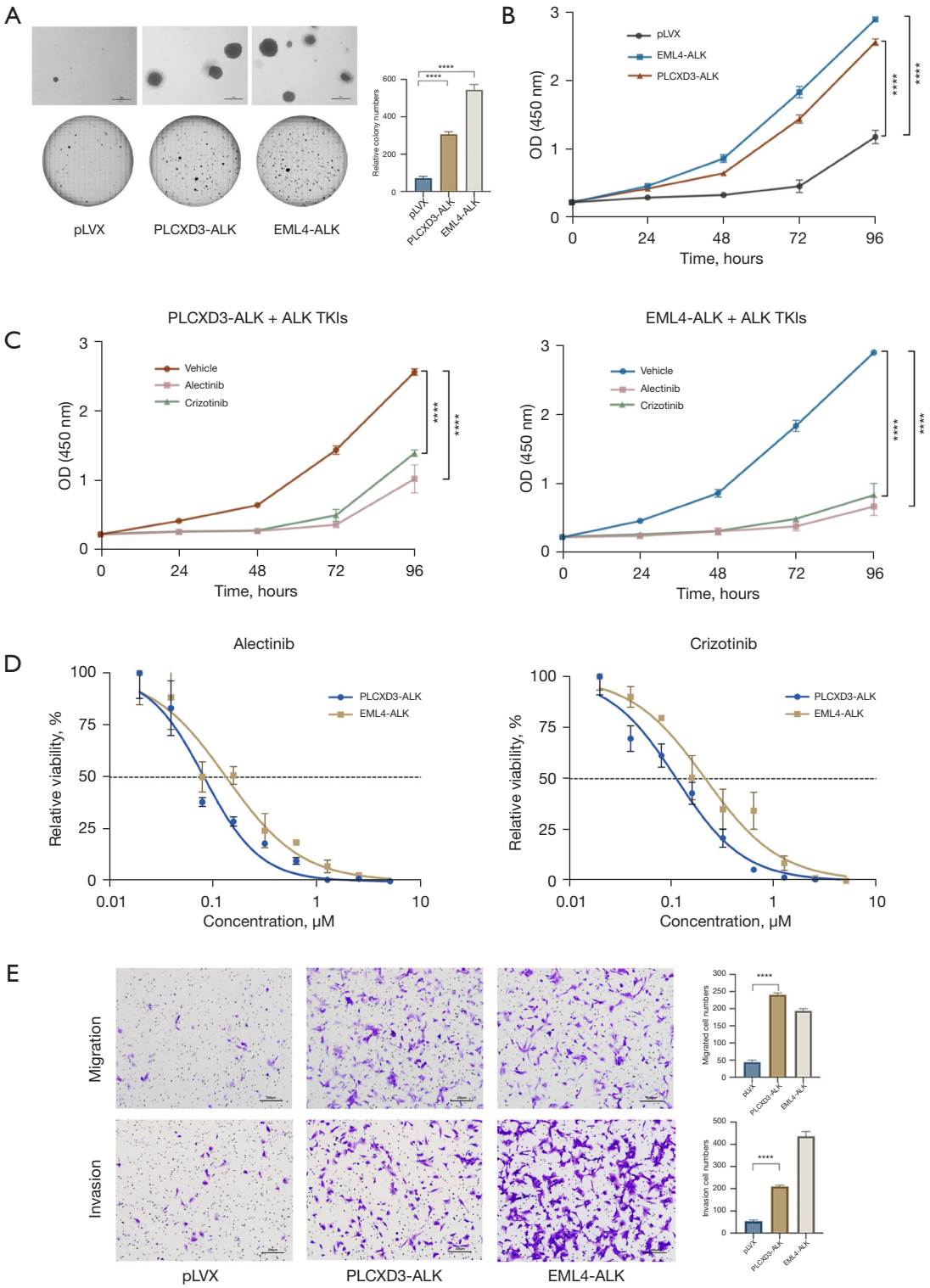

Figure 3 Oncogenic properties of *PLCXD3-ALK*. (A) Increased colony formation in a soft agar assay of NIH-3T3 cells expressing *PLCXD3-ALK* compared with cells expressing *EML4-ALK* or pLVX vector only (mock). The scanned images of the resulting colonies are shown. (B) The effect of expressing PLCXD3-ALK or EML4-ALK on cell proliferation. (C) Cell proliferation was inhibited by the small-molecule ALK TKIs, crizotinib and alectinib. Cell growth curves of the indicated groups by cell counting kit-8 assay. The OD was measured at 450 nm

using a microplate reader. Experiments were performed in triplicate. Two-way ANOVA was used to statistically analyze growth rate (B) and cell viability (C) between groups. (D) NIH-3T3 cells expressing *PLCXD3-ALK* or *EML4-ALK* were cultured in the absence or presence of crizotinib or alectinib at indicated concentrations. Cell viability was determined by cell counting kit-8 assay (450 nm). (E) Cell migration and invasion through a transwell chamber of the indicated groups and their associated quantification. The migrated or invaded cells were stained with crystal violet. Data shown are representative of three independent experiments presented as mean ± standard error of the mean. ****, P<0.0001. ALK, anaplastic lymphoma kinase; TKIs, tyrosine kinase inhibitors; OD, optical density; ANOVA, analysis of variance.

(*Figure 3E*). Then, after treating the cells with crizotinib or alectinib for 24 hours, we assessed the impact of these inhibitors on the ALK signaling pathway. The results indicated that treatment of *PLCXD3-ALK*-transfected cells and *EML4-ALK*-transfected cells with ALK TKIs (crizotinib and alectinib) resulted in the decrease of phosphorylated ALK. Following cell starvation treatment, the use of inhibitors significantly reduced the phosphorylation levels of downstream targets, including ERK, AKT, and STAT3 (*Figure 4*). The data suggested that *PLCXD3-ALK* could conduct self-phosphorylation and further activate downstream signaling pathways.

Tumorigenicity of PLCXD3-ALK in vivo and the ALK TKIs inhibites tumor growth in a PLCXD3-ALK xenograft model

We further evaluated the tumorigenicity of the *PLCXD3-ALK* mutants by inoculating PLCXD3-ALK/3T3 cells, EML4-ALK/3T3 cells, and control vector-transfected NIH-3T3 cells into nude mice, respectively. The *PLCXD3-ALK* group formed subcutaneous tumors in 8 days after inoculation (15 out of 15 inoculations), whereas the mock (cells transfected with pLVX vector only) did not (0 out of 5 inoculations) (*Figure 5A*). After oral treatment with crizotinib (50 mg/kg/2 days) or alectinib (20 mg/kg/2 days), tumor growth was significantly inhibited. Compared to the control group, mice treated with ALK TKIs showed a marked reduction in tumor volume and mass by the end of the study (day 15) (*Figure 5B-5D*).

PLCXD3-ALK represents a potential therapeutic target

Upon identifying the *PLCXD3-ALK* fusion in the patient's tumor and observing its structural similarity to other defined *ALK* fusions, the patient was orally administered alectinib, twice per day at a dose of 600 mg. After 1 month of treatment, there was a significant reduction in the size of the lung tumor mass and the surrounding obstructive inflammation. As treatment continued, follow-up chest CT scans showed further reduction in the lesion area. Efficacy evaluation in accordance with RECIST was partial response (PR) (*Figure 5E*). However, after 6 months into treatment, the CT scan showed little change in tumor size (*Figure 5E*), and multiple metastatic lesions were observed in the brain via magnetic resonance imaging (MRI). Soon after, the patient developed prominent symptoms of brain metastasis. The pathology indicated that the metastasis was from lung cancer, further confirming the development of alectinib resistance. Subsequently, the patient was switched to lorlatinib, a more potent third-generation ALK TKI, for treatment and the patient is currently under follow-up.

Discussion

The *ALK* gene is located on chromosome 2p23.2 and encodes an enzymatic protein known as ALK tyrosine kinase receptor or CD246. This protein consists of an extracellular domain [19–1038], a hydrophobic stretch corresponding to a single-pass transmembrane region [1039–1059], and an intracellular kinase domain [1060–1620] (17). In NSCLC, the fusion mutation of *ALK* is a crucial biological feature, which forms complex dimerization with other multiple protein fragments (18). Novel rare *ALK* fusion partner genes (e.g., *SLC34A2*, *LIMS1*, and *SDK1*) continue to be discovered recently. This diversity of fusion proteins endows tumor cells with unique biological characteristics, thereby affecting the clinical treatment response of patients. Previous research has found that different *ALK* fusion mutations correspond to varying sensitivities to ALK TKIs. These inhibitors were designed to target *ALK* activity, but only the *ALK* activation caused by specific fusion mutations can be effectively inhibited by these drugs (19). In this research, we identified a novel *ALK* fusion partner, *PLCXD3*, which was found on chromosome 5 (5p13.1). Phosphoinositide-specific phospholipase C (PLC) plays a key role in initiating signal transduction and generating two secondary messengers including inositol 1,4,5-trisphosphate (IP3) and diacylglycerol (DAG) (20). Depending on their structure and activation mechanism, PLC isozymes are

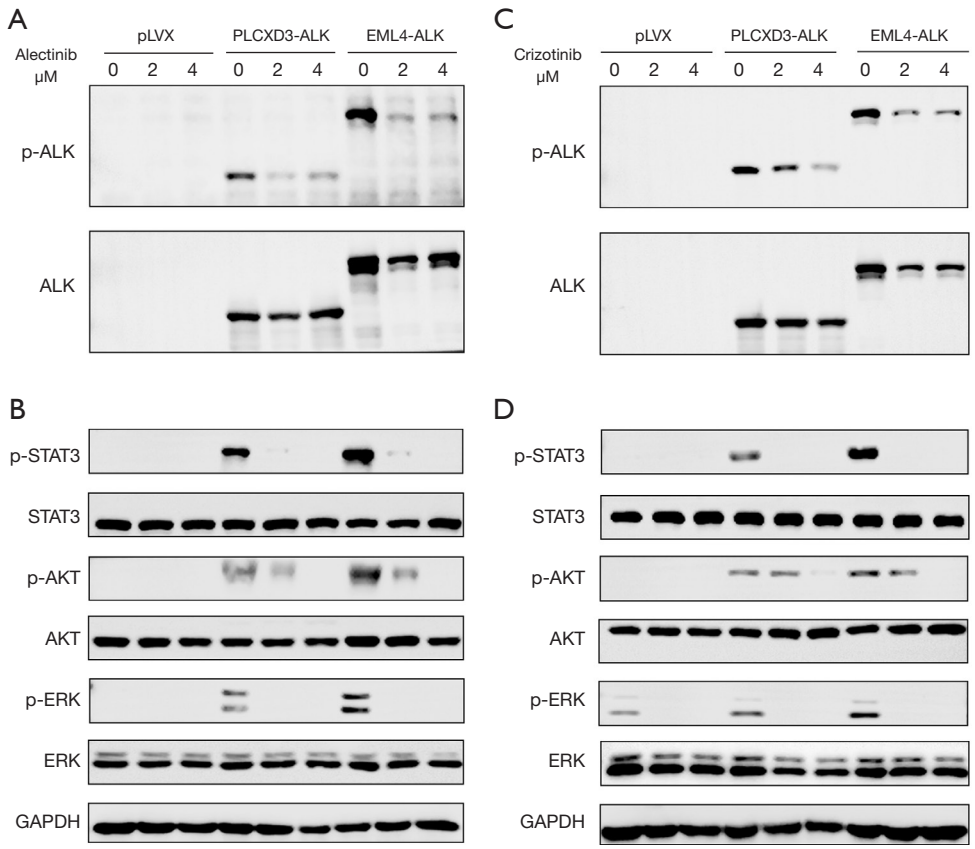

Figure 4 The decrease of phosphorylated ALK and its downstream targets by ALK TKIs. (A) The changes in ALK autophosphorylation levels and (B) the phosphorylation levels of downstream STAT3, AKT, and ERK after treatment with DMSO (vehicle control) or alectinib. (C) The changes in ALK autophosphorylation levels and (D) the phosphorylation levels of downstream STAT3, AKT, and ERK after treatment with DMSO (vehicle control) or crizotinib. Cell lysates were subjected to SDS-PAGE and immunoblotting analysis with specific antibodies as indicated. Results shown are representative of two independent experiments. ALK, anaplastic lymphoma kinase; p-, phosphorylated-; GADPH, glyceraldehyde 3-phosphate dehydrogenase; TKIs, tyrosine kinase inhibitors; DMSO, dimethyl sulfoxide; SDS-PAGE, sodium dodecyl sulfate-polyacrylamide gel electrophoresis.

divided into several subclasses. *PLCXD3*, also known as PI-PLC X domain-containing protein 3, is a protein composed of 321 amino acids and contains a PI-PLC X-box domain which is conserved in many PLC isozymes from prokaryotes to mammals. The X-box domain is essential for the catalytic activity of PLC proteins. *PLCXD3* is a target of D5S430, which is a potential prognostic marker for the survival of patients with the rectal tumor who have not received preoperative treatment (21). The fusion partners of *ALK* play a pivotal role in mediating dimerization and constituting the ALK signaling pathway. For example, nucleophosmin (*NPM*) and *EML4* can mediate ligand-independent dimerization of the ALK fusion proteins, which leads to the activation of the protein kinase domain (22). Besides, these fusion partners possess a coiled-coil structure, which is also a factor contributing to the constitutive activation of their intracellular kinase domains in various malignant tumors (23). In the NIH-3T3 cells stably expressing the *PLCXD3-ALK* fusion, ALK underwent self-phosphorylation, which was similar to that observed in cells expressing *EML4-ALK*. We also investigated the carcinogenic potential of *PLCXD3-ALK* and revealed that cells expressing *PLCXD3-ALK* demonstrated a marked augmentation in colony formation compared to cells transfected with the control vector. Previous investigations have revealed that the administration of ALK inhibitors effectively inhibits the proliferation and induces apoptosis in NSCLC cell lines expressing the *EML4-ALK* (24). Our

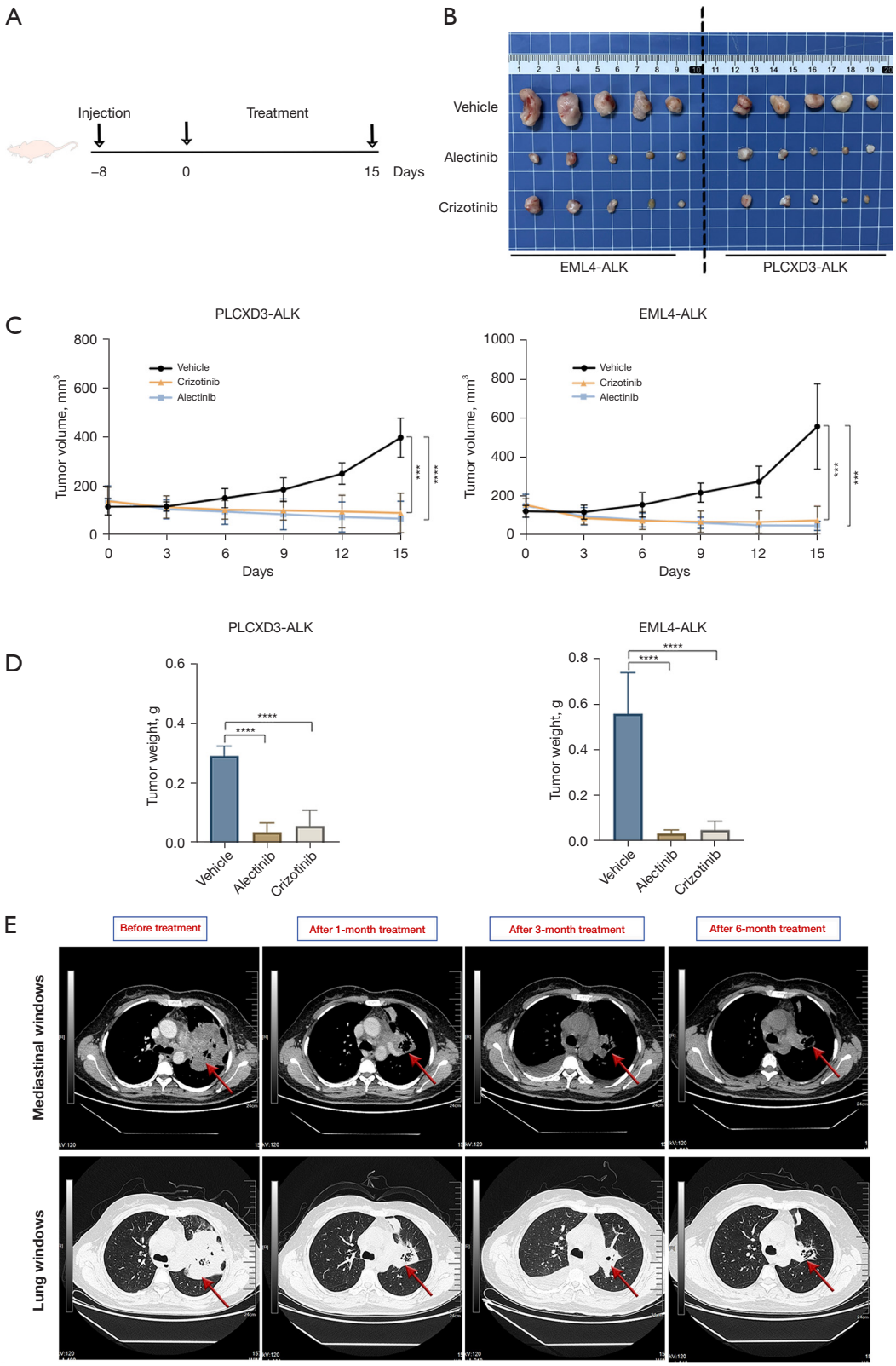

Figure 5 Tumorigenicity of *PLCXD3-ALK in vivo* and inhibition of tumor growth by ALK TKIs. (A) Diagram of mice experiment. (B) Mice were treated with vehicle (n=5), crizotinib (n=5), or alectinib (n=5). (C) Quantification of tumor volume over time. (D) Quantification of

final tumor weight. (E) Radiological features before and after therapy. The CT scans of the patient before therapy and after approximately 1, 3, and 6 months of treatment with alectinib. PR is typically defined as a reduction in tumor size by at least 30, with this reduction being sustained for a period. The region indicated by the arrow represents the tumor mass identified on the CT scan. ***, P<0.001; ****, P<0.0001. ALK, anaplastic lymphoma kinase; TKIs, tyrosine kinase inhibitors; CT, computed tomography; PR, partial response.

study further indicated that the application of ALK kinase inhibitors, including crizotinib and alectinib, significantly impaired the proliferative potential of PLCXD3-ALK/3T3 cells. Concurrently, the treatment significantly diminished the phosphorylation of downstream signaling pathways, including ERK, AKT, and STAT3 in NIH-3T3 cells stably expressing *PLCXD3-ALK*, which confirmed that JAK/STAT3, PI3K/AKT, and RAS/MAPK signaling pathways functioned as the downstream targets of *PLCXD3-ALK*. The oncogenic potential of the *PLCXD3-ALK* mutant was also evaluated *in vivo*. NIH-3T3 cells stably transfected with the *PLCXD3-ALK* mutant demonstrated a significantly increased tumor-forming capacity. Furthermore, similar to the EML4-ALK group, the tumor volume in the PLCXD3-ALK group significantly decreased after treatment with crizotinib and alectinib.

Researches had shown that *ALK* gene rearrangements were predominantly encountered in lung adenocarcinomas, while *ALK*$^+$ LUSC represented a comparatively rare subset (25). A previous cohort study on Asian patients had demonstrated that *ALK* gene fusion mutations were extremely rare in LUSC, with an incidence rate of only 0.2–2.5 (26). Similarly, in the *ALK* fusions that we have summarized, the pathological type was mostly lung adenocarcinoma (*Table 1*). Further observation of treatment efficacy revealed that patients with *ALK*-mutated LUSC exhibited significantly shorter progression-free survival (PFS) when treated with ALK TKIs, compared to the patients treated with similar agents (27). In a single-center study involving 31 patients with *ALK*$^+$ LUSC, 20 patients received ALK inhibitors as first- or second-line therapy. The median PFS was 6.4±4.4 months, which was significantly lower than the efficacy observed with ALK inhibitors in *ALK*-positive lung adenocarcinoma patients (28). Another study involving six patients with LUSC harboring an *EML4-ALK* rearrangement reported a PFS of 2.8 months (range, 1.8–6.3 months) and an overall survival (OS) of 8.3 months (range, 3.2–32.1 months) for those treated with ALK inhibitors as first- or second-line therapy (29). Our study, which included a patient with the *PLCXD3-ALK* fusion mutation (P1, A19), produced similar results. Although the PFS for this LUSC patient treated with ALK inhibitors was approximately 6 months, we confirmed that *PLCXD3-ALK* is a target sensitive to ALK inhibitors. In the future, *PLCXD3-ALK* could be considered a robust fusion mutation comparable to *EML4-ALK* in lung adenocarcinoma patients. We plan to further collect data on lung adenocarcinoma patients with the *PLCXD3-ALK* fusion mutation and conduct functional validation to confirm the role of *PLCXD3-ALK*.

Until now, despite that iterative generations of ALK TKIs have achieved some success, the durability of response remains limited by drug resistance (30). Approximately half of patients with *ALK*$^+$ NSCLC who receive first-line alectinib treatment will experience a relapse, which is an unfortunate but anticipated consequence of tumor evolution and drug resistance development. The molecular mechanisms of resistance to ALK-TKIs can be roughly divided into two categories: one is related to target gene mutations, such as *ALK* resistance mutations and *ALK* gene amplification, the other is the abnormal activation of signaling pathways such as EGFR, KIT, IGF-1R, SRC, MEK/ERK (31). According to previous research, *ALK* G1202R is the most common resistance mutation in *ALK* after treatment with second-generation ALK inhibitors. In addition, other *ALK* resistance mutations including I1171T/S, V1180L, and L1196M also account for a certain proportion. However, for the case reported in our research, no NGS of the tumor tissue and circulating tumor DNA (ctDNA) monitoring were performed after relapse, so whether this patient had resistance mutations remained unknown. In this study, we validated the functional characteristics of PLCXD3-ALK through *in vitro* and *in vivo* experiments, establishing it as a viable therapeutic target for ALK inhibitors. However, we did not directly assess the activity of the ALK kinase domain, and the observed treatment outcome was limited to a 6-month follow-up for this patient. In future work, we plan to continue monitoring the patient's clinical progression and further investigate this novel ALK fusion to provide additional evidence for its inclusion in clinical diagnostic and targeted therapy protocols.

Conclusions

In summary, our study confirmed that the novel ALK fusion, PLCXD3-ALK, displayed similar functional characteristics to the EML4-ALK fusion protein. Consistent results from *in vitro* functional studies and clinical observations suggest that this fusion gene is a viable therapeutic target for ALK inhibitors. Therefore, incorporating *PLCXD3-ALK* into clinical diagnosis and targeted therapy protocols would be beneficial.

Acknowledgments

None.

Footnote

Reporting Checklist: The authors have completed the ARRIVE reporting checklist. Available at https://jtd.amegroups.com/article/view/10.21037/jtd-24-1428/rc

Data Sharing Statement: Available at https://jtd.amegroups.com/article/view/10.21037/jtd-24-1428/dss

Peer Review File: Available at https://jtd.amegroups.com/article/view/10.21037/jtd-24-1428/prf

Funding: This present research was funded by the National Natural Science Foundation of China (to R.J.) (No. 82172620).

Conflicts of Interest: All authors have completed the ICMJE uniform disclosure form (available at https://jtd.amegroups.com/article/view/10.21037/jtd-24-1428/coif). R.J. received funding from the National Natural Science Foundation of China (No. 82172620). The other authors have no conflicts of interest to declare.

Ethical Statement: The authors are accountable for all aspects of the work in ensuring that questions related to the accuracy or integrity of any part of the work are appropriately investigated and resolved. The study was conducted in accordance with the Declaration of Helsinki (as revised in 2013). The study was approved by the Ethics Committee of Tianjin Medical University Cancer Institute and Hospital (No. bc20240063) and informed consent was taken from the patient. Experiments were performed under a project license (No. 2024006) granted by the Animal Care and Use Committee of Tianjin Medical University Cancer Institute and Hospital, in compliance with institutional guidelines for the care and use of animals.

References

1. Herbst RS, Morgensztern D, Boshoff C. The biology and management of non-small cell lung cancer. Nature 2018;553:446-54.
2. Wu W, Haderk F, Bivona TG. Non-Canonical Thinking for Targeting ALK-Fusion Onco-Proteins in Lung Cancer. Cancers (Basel) 2017;9:164.
3. Armstrong F, Duplantier MM, Trempat P, et al. Differential effects of X-ALK fusion proteins on proliferation, transformation, and invasion properties of NIH3T3 cells. Oncogene 2004;23:6071-82.
4. Wu J, Hu Y, Abdihamid O, et al. Crizotinib in Sarcomatous Malignancies Harboring ALK Fusion With a Definitive Partner(s): Response and Efficacy. Front Oncol 2021;11:684865.
5. Tabbò F, Muscarella LA, Gobbini E, et al. Detection of ALK fusion variants by RNA-based NGS and clinical outcome correlation in NSCLC patients treated with ALK-TKI sequences. Eur J Cancer 2022;174:200-11.
6. Patcas A, Chis AF, Militaru CF, et al. An insight into lung cancer: a comprehensive review exploring ALK TKI and mechanisms of resistance. Bosn J Basic Med Sci 2022;22:1-13.
7. Shaw AT, Bauer TM, de Marinis F, et al. First-Line Lorlatinib or Crizotinib in Advanced ALK-Positive Lung Cancer. N Engl J Med 2020;383:2018-29.
8. Shaw AT, Solomon BJ, Besse B, et al. ALK Resistance Mutations and Efficacy of Lorlatinib in Advanced Anaplastic Lymphoma Kinase-Positive Non-Small-Cell Lung Cancer. J Clin Oncol 2019;37:1370-9.
9. Camidge DR, Kim HR, Ahn MJ, et al. Brigatinib Versus Crizotinib in Advanced ALK Inhibitor-Naive ALK-Positive Non-Small Cell Lung Cancer: Second Interim

Analysis of the Phase III ALTA-1L Trial. J Clin Oncol 2020;38:3592-603.
10. Ou SI, Lee ATM, Nagasaka M. From preclinical efficacy to 2022 (36.7 months median follow -up) updated CROWN trial, lorlatinib is the preferred 1st-line treatment of advanced ALK+ NSCLC. Crit Rev Oncol Hematol 2023;187:104019.
11. Lin JJ, Horan JC, Tangpeerachaikul A, et al. NVL-655 Is a Selective and Brain-Penetrant Inhibitor of Diverse ALK-Mutant Oncoproteins, Including Lorlatinib-Resistant Compound Mutations. Cancer Discov 2024;14:2367-86.
12. Ou SI, Zhu VW, Nagasaka M. Catalog of 5' Fusion Partners in ALK-positive NSCLC Circa 2020. JTO Clin Res Rep 2020;1:100015.
13. Xin P, Xu X, Deng C, et al. The role of JAK/STAT signaling pathway and its inhibitors in diseases. Int Immunopharmacol 2020;80:106210.
14. Yu L, Wei J, Liu P. Attacking the PI3K/Akt/mTOR signaling pathway for targeted therapeutic treatment in human cancer. Semin Cancer Biol 2022;85:69-94.
15. Santarpia L, Lippman SM, El-Naggar AK. Targeting the MAPK-RAS-RAF signaling pathway in cancer therapy. Expert Opin Ther Targets 2012;16:103-19.
16. Kilkenny C, Browne WJ, Cuthill IC, et al. Improving bioscience research reporting: the ARRIVE guidelines for reporting animal research. PLoS Biol 2010;8:e1000412.
17. Hallberg B, Palmer RH. The role of the ALK receptor in cancer biology. Ann Oncol 2016;27 Suppl 3:iii4-iii15.
18. Takeuchi K, Soda M, Togashi Y, et al. RET, ROS1 and ALK fusions in lung cancer. Nat Med 2012;18:378-81.
19. Zhao S, Li J, Xia Q, et al. New perspectives for targeting therapy in ALK-positive human cancers. Oncogene 2023;42:1959-69.
20. Gellatly SA, Kalujnaia S, Cramb G. Cloning, tissue distribution and sub-cellular localisation of phospholipase C X-domain containing protein (PLCXD) isoforms. Biochem Biophys Res Commun 2012;424:651-6.
21. Romain B, Neuville A, Meyer N, et al. Allelotyping identification of genomic alterations in rectal chromosomally unstable tumors without preoperative treatment. BMC Cancer 2010;10:561.
22. Schneider JL, Lin JJ, Shaw AT. ALK-positive lung cancer: a moving target. Nat Cancer 2023;4:330-43.
23. Amano Y, Ishikawa R, Sakatani T, et al. Oncogenic TPM3-ALK activation requires dimerization through the coiled-coil structure of TPM3. Biochem Biophys Res Commun 2015;457:457-60.
24. Zhang SS, Nagasaka M, Zhu VW, et al. Going beneath the tip of the iceberg. Identifying and understanding EML4-ALK variants and TP53 mutations to optimize treatment of ALK fusion positive (ALK+) NSCLC. Lung Cancer 2021;158:126-36.
25. Wang J, Shen Q, Shi Q, et al. Detection of ALK protein expression in lung squamous cell carcinomas by immunohistochemistry. J Exp Clin Cancer Res 2014;33:109.
26. Caliò A, Nottegar A, Gilioli E, et al. ALK/EML4 fusion gene may be found in pure squamous carcinoma of the lung. J Thorac Oncol 2014;9:729-32.
27. Watanabe J, Togo S, Sumiyoshi I, et al. Clinical features of squamous cell lung cancer with anaplastic lymphoma kinase (ALK)-rearrangement: a retrospective analysis and review. Oncotarget 2018;9:24000-13.
28. Meng Q, Dong Y, Tao H, et al. ALK-rearranged squamous cell carcinoma of the lung. Thorac Cancer 2021;12:1106-14.
29. Lewis WE, Hong L, Mott FE, et al. Efficacy of Targeted Inhibitors in Metastatic Lung Squamous Cell Carcinoma With EGFR or ALK Alterations. JTO Clin Res Rep 2021;2:100237.
30. He L, Dar AC. Targeting drug-resistant mutations in ALK. Nat Cancer 2022;3:659-61.
31. Gainor JF, Dardaei L, Yoda S, et al. Molecular Mechanisms of Resistance to First- and Second-Generation ALK Inhibitors in ALK-Rearranged Lung Cancer. Cancer Discov 2016;6:1118-33.

Cite this article as: Chen K, Chen X, Wang X, Yan B, Liu A, Wang Y, Zhou J, Wei Q, Pan Y, Jiang R. *PLCXD3-ALK*, a novel *ALK* rearrangement in lung squamous cell carcinoma and its clinical responses to ALK inhibitors. J Thorac Dis 2025;17(1):93-108. doi: 10.21037/jtd-24-1428